# A simple model for nuclear modification of parton distribution functions*

A.V. Kotikov[1] A.V. Lipatov[2]

[1]Joint Institute for Nuclear Research, 141980 Dubna, Moscow region, Russia
[2]Skobeltsyn Institute of Nuclear Physics, Lomonosov Moscow State University, 119991 Moscow, Russia

**Abstract:** A model for the nuclear medium modification of parton densities is presented. The approach is based on a global analysis of available deep inelastic scattering data for different nuclear targets within the rescaling model, combined with the effects of Fermi motion. The scale dependence is implemented through the DGLAP-evolved quark and gluon densities in a proton derived analytically at the leading order of QCD coupling. By fitting the rescaling parameters to experimental data on the ratio $F_2^A(x,Q^2)/F_2^{A'}(x,Q^2)$ for several nuclear targets $A$ and $A'$, we obtain predictions for nuclear parton distributions, even for unmeasured nuclei. The effects of nuclear modifications are investigated with respect to the mass number $A$. We highlight distinct shadowing and antishadowing behaviors for gluons and quarks.

**Keywords:** deep inelastic scattering, parton densities in a proton and nuclei, EMC effect

**DOI:** 10.1088/1674-1137/ae25ca **CSTR:** 32044.14.ChinesePhysicsC.50034109

## I. INTRODUCTION

The study of deep inelastic scattering (DIS) of leptons on nuclei shows significant effects of nucleon interactions within the nucleus, challenging a naive picture of the nucleus as a system of quasi-free nucleons (see reviews [1−4]). Nuclear medium effects on parton (quark and gluon) distribution functions (PDFs) attract considerable interest from both experimental and theoretical perspectives [5−20]. In particular, a detailed understanding of nuclear modifications of the parton densities (nPDFs) is a fundamental problem of nuclear and high energy physics at present, and it is crucial for any theoretical description of $pA$ and $AA$ collisions at modern (LHC and RHIC) and future colliders (FCC-he, EiC, EicC, CEPC, and NICA). Usually, the nuclear modification factor is defined as a ratio of per-nucleon DIS structure functions in nucleus $A$ and deuteron[1)] $D$, $R^A = F_2^A(x,Q^2)/F_2^D(x,Q^2)$, or the ratio of the corresponding parton densities, which is introduced to investigate the behavior across different kinematic regions: shadowing ($x \leqslant 0.1$), anti-shadowing ($0.1 \leqslant x \leqslant 0.3$), valence quark dominance ($0.3 \leqslant x \leqslant 0.7$), and Fermi motion ($x \geqslant 0.7$). The shadowing ($R_A < 1$) and anti-shadowing ($R_A > 1$) effects refer to the suppression or enhancement of the structure function ratios, while the EMC effect [26] and Fermi motion influence the slope of $R_A$ in the valence-dominated region and its rise at larger $x$. Note that the nuclear medium effect was first discovered [26] by the European Muon Collaboration (EMC) in the domain of valence quark dominance. The investigations on shadowing and antishadowing (see [27−31]) started before the availability of the EMC experimental data [6, 7] (see also [32] for an overview). Moreover, antishadowing as a phenomenon was introduced [29, 30].

Unfortunately, at present, there is no commonly recognized framework to describe nuclear PDF modifications over the entire kinematical range of $x$, as well as the corresponding nuclear dependence. Two main approaches exist: global fits to nuclear data using empirical starting nPDFs followed by the standard Dokshitzer-Gribov-Lipatov-Altarelli-Parisi (DGLAP) equations [33−36] to describe their scale dependence (see recent studies [23, 24, 37−41] and references therein) and model-based approaches (see, for example, [25, 42] and discussions therein). The first technique is analogous to employing the standard derivation of the PDFs (see review [4]). Models of nuclear medium modifications can be roughly divided into two categories: models based on conventional nuclear physics and models inspired by QCD (see [42]). The first type typically considers the decrease in the nucleon mass in the medium, leading to the so-called

Received 10 October 2025; Accepted 26 November 2025; Accepted manuscript online 27 November 2025

* This research has been carried out at the expense of the Russian Science Foundation grant 25-22-00066, https://rscf.ru/en/project/25-22-00066/

1) Assuming that the nuclear effects in deutron are negligible, so the deuteron is considered as a system of a free proton and neutron. We note, however, that studies of nuclear effects in the deuteron can be found [21−24]. See also discussions [25]

$x$-rescaling models [43−48] and off-shellness corrections [49−53]. The QCD-inspired models typically require an increase in quark confinement or a simple increase in the nucleon radius (nucleon swelling [23, 42]). A larger nucleon corresponds to a higher probe resolution. In terms of QCD evolution, $Q^2$-rescaling [54−60] is used to interpret the effect. All these analyses [23, 24, 37, 38, 52, 53, 57, 58, 59, 61, 62] have shown remarkable progress in the last decade. Nevertheless, quark and especially gluon densities in nuclei still have large uncertainties across the entire $x$ region due to a shortage of experimental data and/or limited kinematic coverage of the latter [63−65].

In the framework of the $Q^2$-rescaling model (everywhere below —rescaling model), the nuclear medium modification was investigated [54, 56, 57, 58, 59]. Initially, this model was proposed for the valence-dominant region, and it is based on the suggestion that the effective confinement size of gluons and quarks in the nucleus is greater than in the free nucleon. Such a shift in the confinement scale results in relation between the PDFs and nPDFs through a simple rescaling of their arguments [57, 58, 59, 61, 62]. Thus, the rescaling model demonstrates the features inherent in both approaches: a connection exists between PDFs and nPDFs arising due to the shift in the scale and, at the same time, both PDFs and nPDFs obey the DGLAP equations. Relatively recently, the rescaling model has been extended to the low $x$ range [54] (note that, in the framework of the $x$-rescaling model, the low $x$ range was first investigated [66]). It was shown [54, 56, 67] that good agreement with available experimental data on $F_2^A(x,Q^2)/F_2^D(x,Q^2)$ ratios at low and moderate $x$ could be achieved by fitting the corresponding rescaling parameters.

The aim of this study is to extend and improve earlier considerations [54, 56]. Firstly, we employ updated analytical expressions for PDFs obtained very recently [68] from the solution of the DGLAP evolution equations at the leading order (LO) of QCD coupling. These expressions rely on exact asymptotics at small and large $x$ and contain subasymptotic terms that are fixed by momentum conservation and/or the Gross-Llewellyn-Smith and Gottfried sum rules. Some phenomenological parameters have been determined from a rigorous fit to precision BCDMS, H1, and ZEUS experimental data on the proton structure function $F_2(x,Q^2)$ in a wide kinematical region, with $2\cdot10^{-5}\leqslant x\leqslant 0.75$ and $1.2\leqslant Q^2\leqslant 30000$ GeV$^2$. This is in contrast with previous studies [54, 56], where only low-$x$ asymptotics were considered. The second improvement is related to the Fermi motion. The latter is necessary to provide a consistent description of nuclear modifications across the entire kinematic range. Thirdly, to extract the rescaling parameters, we perform a global fit to available experimental data on the ratios $F_2^A(x,Q^2)/F_2^{A'}(x,Q^2)$ for different nuclear targets $A$ and $A'$ collected by the EMC [5−8], NMC [9−13], SLAC [14], BCDMS [15, 16], E665 [17, 18], JLab [19], and CLAS [20] Collaborations. Then, we investigate the dependence of our results on the mass number $A$, derive predictions for the corresponding nuclear parton distributions in a simple analytical form, and investigate the effects of nuclear modifications. Thus, our present study is a continuation of previous investigations [54, 56, 68].

The rest of our paper is organized as follows. In Sec. II, we list small-$x$ and large-$x$ asymptotics, which are used to construct the PDFs in the entire kinematical region. In Sec. III, we recall the basic formulas of the rescaling model and extend it with Fermi motion. Section IV presents our numerical results and discussions. Section V contains our conclusions. In Appendix A, we present the basic elements of the rescaling model [57−62].

## II. STRUCTURE FUNCTION $F_2(x,Q^2)$ AND PARTON DENSITIES IN A PROTON

We start from some basic formulas used in our calculations. It is well known that the proton structure function $F_2(x,Q^2)$ at LO of QCD coupling can be expressed as

$$F_2(x,Q^2)=\sum_{i=1}^{N_f}e_i^2\left[f_{q_i}(x,Q^2)+f_{\bar{q}_i}(x,Q^2)\right], \tag{1}$$

where $e_i$ is the fractional electric charge of quark $q_i$, $N_f$ is the number of active quark flavors, and $f_{q_i}(x,Q^2)$ and $f_{\bar{q}_i}(x,Q^2)$ represent the quark and antiquark densities in a proton (multiplied by $x$), respectively. In the fixed-flavor-number-sheme (FFNS) with $N_f=4$, where $b$ and $t$ quarks are separated out, we have

$$F_2(x,Q^2)=\frac{5}{18}f_{S1}(x,Q^2)+\frac{1}{6}f_{NS}(x,Q^2), \tag{2}$$

where the singlet part $f_{S1}(x,Q^2)$ contains the valence $f_V(x,Q^2)$ and sea $f_S(x,Q^2)$ quark parts:

$$\begin{aligned}
f_V(x,Q^2)&=f_u^V(x,Q^2)+f_d^V(x,Q^2),\\
f_S(x,Q^2)&=\sum_{i=1}^{4}\left[f_{q_i}^S(x,Q^2)+f_{\bar{q}_i}^S(x,Q^2)\right],\\
f_{S1}(x,Q^2)&=\sum_{i=1}^{4}\left[f_{q_i}(x,Q^2)+f_{\bar{q}_i}(x,Q^2)\right]\\
&=f_V(x,Q^2)+f_S(x,Q^2).
\end{aligned} \tag{3}$$

The nonsinglet part $f_{NS}(x,Q^2)$ contains the difference between up and down quarks:

$$f_{NS}(x,Q^2) = \sum_{q=u,c}\left[f_q(x,Q^2)+f_{\bar{q}}(x,Q^2)\right] - \sum_{q=d,s}\left[f_q(x,Q^2)+f_{\bar{q}}(x,Q^2)\right]. \quad (4)$$

The non-singlet and valence parts of quark distribution functions can be represented in the following form [68, 69] (see also [70, 71]):

$$f_i(x,\mu^2) = \left[A_i(s)x^{\lambda_i}(1-x)+\frac{B_i(s)\,x}{\Gamma(1+\nu_i(s))} + D_i(s)x(1-x)\right](1-x)^{\nu_i(s)}, \quad (5)$$

where $i = NS$ or $V$, $s = \ln\left[\alpha_s(Q_0^2)/\alpha_s(Q^2)\right]$ and

$$A_i(s) = A_i(0)\mathrm{e}^{-d(n_i)s},\ \ B_i(s) = B_i(0)\mathrm{e}^{-ps},$$
$$\nu_i(s) = \nu_i(0)+rs,\ \ r = \frac{16}{3\beta_0},\ \ p = r(\gamma_{\rm E}+\hat{c}),$$
$$\hat{c} = -\frac{3}{4},\ \ d(n) = \frac{\gamma_{NS}(n)}{2\beta_0},\ \ n_i = 1-\lambda_i. \quad (6)$$

Here, $\Gamma(z)$ is the Riemann's $\Gamma$-function; $\gamma_{\rm E}\simeq 0.5772$ is the Euler's constant; $\beta_0 = 11-2N_f/3$ is the LO QCD $\beta$-function; $\lambda_{NS} = \lambda_V = 0.5$; $\gamma_{NS}(n)$ is the LO non-singlet anomalous dimension; and $A_i(0)$, $B_i(0)$, and $\nu_i(0)$ are the free parameters. Note that Eq. (5) is constructed as a combination of the small-$x$ part proportional to $A_i(s)$, large-$x$ asymptotic part proportional to $B_i(s)$, and an additional term proportional to $D_i(s)$. The latter is subasymptotic in both these regions, and its scale dependence is fixed by the Gross-Llewellyn-Smith and Gottfreed sum rules [68, 69]:

$$D_i(s) = (2+\nu_i(s))\left[N_i - A_i(s)\frac{\Gamma(\lambda_i)\Gamma(2+\nu_i(s))}{\Gamma(\lambda_i+2+\nu_i(s))} - \frac{B_i(s)}{\Gamma(2+\nu_i(s))}\right], \quad (7)$$

where $N_V = 3$ and [72] (see [68] and references therein for more information)

$$N_{NS} \equiv I_G(Q^2) = 0.705\pm 0.078. \quad (8)$$

Based on [68] (see also [73]), we use the result of Eq. (8) for $I_G(Q^2)$, which is very different from the theoretical prediction $I_G(Q^2) = 1$ based on the quark sea symmetry. In principle, such a violation could occur not for partons inside a free nucleon but under nuclear medium modification. We plan to explore this possibility in our future studies.

The singlet part of quark densities and gluon distribution in a proton can be represented as combinations of "±" terms [68, 69] (see also [54, 70]):

$$f_i(x,Q^2) = f_i^+(x,Q^2)+f_i^-(x,Q^2), \quad (9)$$

where $i = SI$ or $g$ (note that, based on [74–77], we exploit the non-Regge behavior for singlet quarks and gluons at small $x$. The corresponding parametrizations with Regge behavior at small $x$ [78, 79] can be found [80]).

$$f_{SI}^+(x,Q^2) = \left[\frac{N_f}{9}\left(A_g+\frac{4}{9}A_q\right)\rho I_1(\sigma)\mathrm{e}^{-\bar{d}^+s}(1-x)^{m_q^+} + D^+(s)\sqrt{x}(1-x)^{n^+} - \frac{K^+}{\Gamma(2+\nu^+(s))} \times \frac{B^+(s)x}{\hat{c}-\ln(1-x)+\Psi(2+\nu^+(s))}\right](1-x)^{\nu^+(s)+1}, \quad (10)$$

$$f_{SI}^-(x,Q^2) = \left[A_q e^{-d^-s}(1-x)^{m_q^-} + \frac{B^-(s)x}{\Gamma(1+\nu^-(s))} + D^-(s)\sqrt{x}(1-x)^{n^-}\right](1-x)^{\nu^-(s)}, \quad (11)$$

$$f_g^+(x,Q^2) = \left[\left(A_g+\frac{4}{9}A_q\right)I_0(\sigma)\mathrm{e}^{-\bar{d}^+s}(1-x)^{m_g^+} + \frac{B^+(s)x}{\Gamma(1+\nu^+(s))}\right](1-x)^{\nu^+(s)}, \quad (12)$$

$$f_g^-(x,Q^2) = \left[-\frac{4}{9}A_q\mathrm{e}^{-d^-s}(1-x)^{m_g^-} + \frac{K^-}{\Gamma(2+\nu^-(s))} \times \frac{B^-(s)x}{\hat{c}-\ln(1-x)+\Psi(2+\nu^-(s))}\right](1-x)^{\nu^-(s)+1}. \quad (13)$$

Here, $\Psi(z)$ is the Riemann's $\Psi$-function, $I_0(z)$ and $I_1(z)$ are the modified Bessel functions, and

$$\nu^\pm(s) = \nu^\pm(0)+r^\pm s,\ \ B^\pm(s) = B^\pm(0)\mathrm{e}^{-p^\pm s},$$
$$p^\pm = r^\pm(\gamma_{\rm E}+\hat{c}^\pm),\ \ r^+ = \frac{12}{\beta_0},\ \ r^- = \frac{16}{3\beta_0},$$
$$\hat{c}^+ = -\frac{\beta_0}{12},\ \ \hat{c}^- = -\frac{3}{4},\ \ K^+ = \frac{3N_f}{10},\ \ K^- = \frac{2}{5},$$
$$\rho = \frac{\sigma}{2\ln(1/x)},\ \ \sigma = 2\sqrt{|\hat{d}^+|s\ln\frac{1}{x}},\ \ \hat{d}^+ = -\frac{12}{\beta_0},$$
$$\bar{d}^+ = 1+\frac{20N_f}{27\beta_0},\ \ d^- = \frac{16N_f}{27\beta_0} \quad (14)$$

with $A_g$, $A_q$, $B^\pm(0)$, $\nu^\pm(0)$, $m_q^\pm$, $m_g^\pm$, and $n^\pm$ being free para-

meters. The expressions for subasymptotic terms $D^{\pm}(s)$ are derived from the momentum conservation law and can be found elsewhere [68]. Note that LO small-$x$ asymptotics in the formulas above were obtained in the so-called generalized doubled asymptotic scaling (DAS) approximation [74–76]. In this approximation, flat initial conditions, $f_g(x,Q_0^2)=A_g$ and $f_S(x,Q_0^2)=A_q$, can be used. All the phenomenological parameters in Eqs. (5)–(13) were determined [68] by fitting the precise data on the proton structure function $F_2(x,Q^2)$.

These expressions are crucial in the subsequent analysis of experimental data on nuclear structure function ratios $F_2^A(x,Q^2)/F_2^{A'}(x,Q^2)$ for different nuclear targets within the framework of the rescaling model.

## III. MODEL OF NUCLEAR MODIFICATIONS

As a model of nuclear modifications of listed above parton densities, we consider the combination of the rescaling model [57, 58, 59] and Fermi motion. So, there is simple relationship between ordinary PDFs and nPDFs via a shift in the kinematical variable $Q^2$ proposed within the rescaling model[1)] (see also [61, 62]). For a nucleus $A$, the valence and nonsinglet parts are modified as:

$$f_i^A(x,Q^2)=f_i(x,Q_{A,i}^2), \tag{15}$$

where $i=V$ or $NS$, and scale $Q_{A,i}^2$ is related to $Q^2$ by

$$s_i^A\equiv\ln\left(\frac{\ln\left(Q_{A,i}^2/\Lambda_{\rm QCD}^2\right)}{\ln\left(Q_0^2/\Lambda_{\rm QCD}^2\right)}\right)=s+\ln\left(1+\delta_i^A\right), \tag{16}$$

with $\delta_i^A$ being the scale independent free parameters (see [54] and references therein) and the analytical expressions for $f_i(x,Q^2)$ given by Eqs. (5) and (6).

Exploiting the fact that parton densities increase with $Q^2$, the rescaling model was extended [54] to low $x$ or the shadowing region. Indeed, if we change the scale in the QCD evolution to be less than $Q^2$, we can immediately reproduce the nuclear shadowing effects observed in the global fits. At low $x$, the singlet part of quark densities and the gluon distribution in a proton are non-negligible, and each of them has two ("+" and "−") independent components. Therefore, we have two additional free parameters to be fit from the nuclear data. Thus,

$$\begin{aligned} f_i^A(x,Q^2)&=f_i^{A,+}(x,Q^2)+f_i^{A,-}(x,Q^2),\\ f_i^{A,\pm}(x,Q^2)&=f_i^{\pm}(x,Q_{A,\pm}^2), \end{aligned} \tag{17}$$

where $i=SI$ or $g$, and the expressions for $f_i^{\pm}(x,Q^2)$ are given by Eqs. (9)–(12). The definition of $Q_{A,\pm}^2$ is the same as that above, and the corresponding values of $s_{\pm}^A$ are [54]

$$s_{\pm}^A\equiv\ln\left(\frac{\ln\left(Q_{A,\pm}^2/\Lambda_{\rm QCD}^2\right)}{\ln\left(Q_0^2/\Lambda_{\rm QCD}^2\right)}\right)=s+\ln\left(1+\delta_{\pm}^A\right). \tag{18}$$

Here, the free parameters $\delta_{\pm}^A$ are scale independent, have to be negative, and can be determined from the available data [54, 56].

Another improvement that was made in this study in comparison with early studies [54, 56] is taking into account the Fermi motion of the nucleon inside the nuclear target. As already mentioned above, Fermi smearing deforms the nuclear structure function mainly at large $x>0.7$. For nonsinglet and valence parts, such deformation can be described by the convolution [81, 82]

$$f_i^{A(F)}(x,Q^2)=\frac{1}{R_{NS}}\int\limits_{y_{\rm min}}^{y_{\rm max}}\frac{{\rm d}y}{y}\left[yf_N(y)\right]f_i^A\left(x/y,Q^2\right), \tag{19}$$

where $i=V$ or $NS$ and

$$\begin{aligned} &f_N(y)=(\eta_+-y)(y-\eta_-),\ \ \eta_{\pm}=1-\frac{B_A}{m_N}\pm s_F,\\ &R_{NS}=\frac{4}{3}s_F^3,\ \ s_F=\frac{k_F}{m_N}. \end{aligned} \tag{20}$$

Here, $m_N$ is the nucleon mass, $k_F\simeq 200$ MeV is the average nucleon Fermi momentum for the nuclei, and $B_A$ is the nuclear binding energy per nucleon. The integration limits are $y_{\rm min}=\max(x,1-B_A/m_N-s_F)$ and $y_{\rm max}=\min(A,1-B_A/m_N+s_F)$. Using Eqs. (19) and (20), we have

$$\int\limits_0^1\frac{{\rm d}x}{x}f_i^{A(F)}(x,Q^2)=\int\limits_0^1\frac{{\rm d}x}{x}f_i^A(x,Q^2)=N_i. \tag{21}$$

Thus, Fermi motion obeys the Gross-Llewellyn-Smith and Gottfreed sum rules. Similarly, for the singlet and gluon parts, we have

$$f_i^{A(F)}(x,Q^2)=\frac{1}{R_{SI}}\int\limits_{y_{\rm min}}^{y_{\rm max}}\frac{{\rm d}y}{y}\left[yf_N(y)\right]f_i^A\left(x/y,Q^2\right), \tag{22}$$

where $i=SI$ or $g$ and

$$R_{SI}=\frac{4}{3}s_F^3\eta. \tag{23}$$

One can easily obtain that

1) A fairly detailed explanation of the main points of the rescaling model is given in Appendix A.

$$\int_0^1 \mathrm{d}x \left[f_{SI}^{A(F)}(x,Q^2)+f_g^{A(F)}(x,Q^2)\right] = \int_0^1 \mathrm{d}x \left[f_{SI}^{A}(x,Q^2)+f_g^{A}(x,Q^2)\right] = 1, \quad (24)$$

and therefore, taking Fermi motion into account is consistent with momentum conservation. The nuclear binding energy $B_A$ is precisely measured [83]. We use the proposed empirical formula [23] to describe the nuclear dependence of the $k_F$:

$$k_F(Z,A) = k_F^p\left(1-A^{-t_1}\right)\frac{Z}{A} + k_F^n\left(1-A^{-t_2}\right)\frac{A-Z}{A}, \quad (25)$$

where $k_F^p = 365$ MeV, $k_F^n = 231$ MeV, $t_1 = 0.479$, $t_2 = 0.528$, and $Z$ and $A$ are the proton and mass numbers, respectively.

Thus, the full model that was described above combines rescaling and Fermi motion effects. Eqs. (15)−(23) and (25), along with the analytical formulas in Eqs. (5)−(13) and the corresponding rescaling parameters $\delta_V^A$, $\delta_{NS}^A$, and $\delta_\pm^A$, provide one with a possibility to evaluate nPDFs for any nuclear target $A$. The nuclear structure functions $F_2^A(x,Q^2)$ as well as their ratios for various nuclei can be calculated in the same way as that for the proton, according to the general formula in Eq. (2). The values of the rescaling parameters are determined below.

## IV. NUMERICAL RESULTS

To extract the rescaling parameters $\delta_V^A$, $\delta_{NS}^A$, and $\delta_\pm^A$ for various nuclear targets we performed a global fit to structure function ratio data taken by the EMC [5−8], NMC [9−13], SLAC [14], BCDMS [15, 16], E665 [17, 18], JLab [19], and CLAS [20] Collaborations. It is important to point out that we impose some kinematical cuts on the experimental data to ensure that the data points are in the deep inelastic region, namely, $Q^2 \geqslant 1$ GeV$^2$ and $W^2 \geqslant 4$ GeV$^2$. During the fit, we suggest that $\delta_V^A = \delta_{NS}^A$. Following [68], we set $\Lambda_{\rm QCD}^{(4)} = 118$ MeV, which corresponds to the world averaged $\alpha_s(M_Z^2) = 0.1180$ [84]. We apply a "frozen" treatment of the QCD coupling in the infrared region (see, for example [85, 86] and references therein), where $\alpha_s(\mu^2) \to \alpha_s(\mu^2+M_\rho^2)$ with $M_\rho \sim 1$ GeV. Such treatment leads to a good description of the data on the proton structure function $F_2(x,Q^2)$ [68].

The results of our fits for various nuclei are summarized in Table 1. The measured nuclear targets involved in the analysis, the number or data points $N$, and the goodness, $\chi^2/n.d.f.$, are also presented. The fitting procedure was performed using the algorithm as implemented in the commonly used GNUPLOT package [87]. One can see that reasonably good values of $\chi^2/n.d.f.$ are achieved in most cases. The newly fitted values of $\delta_+^A$, responsible for nuclear shadowing effects, are very close to the ones obtained earlier [56] via analysis on $^4$He, $^{12}$C, and $^{40}$Ca alone. This is because $\delta_+^A$ fits are mainly sensitive to the low-$x$ data, for which the same PDF asymptotics are used in the both calculations. However, our results for $\delta_-^A$ and $\delta_{NS}^A$, essential for larger $x$ and responsible for the description of the EMC and/or anti-shadowing effects, differ from those of earlier analyses [54, 56]. This difference arises owing to various reasons. First, the present consideration is based on the updated PDFs, which are more accurately determined in a wide region of $x$ and $Q^2$. Second, we took the effects of Fermi motion into account,

**Table 1.** The $\delta_\pm^A$ and $\delta_{NS}^A$ parameters extracted from the EMC [5−8], NMC [9−13], SLAC [14], BCDMS [15, 16], E665 [17, 18], JLab [19] and CLAS [20] data.

| $A$ | $\delta_+^A$ | $\delta_-^A$ | $\delta_{NS}^A$ | Targets | $N$ | $\chi^2/n.d.f.$ |
|---|---|---|---|---|---|---|
| $^4$He | $-0.023 \pm 0.004$ | $-0.017 \pm 0.002$ | $0.17 \pm 0.02$ | $^4$He/$^2$D | 42 | 0.63 |
| $^6$Li | $-0.017 \pm 0.005$ | $-0.014 \pm 0.003$ | $0.29 \pm 0.27$ | $^6$Li/$^2$D | 17 | 1.39 |
| $^6$Li | $-0.015 \pm 0.005$ | $-0.012 \pm 0.002$ | $0.11 \pm 0.12$ | $^{12}$C/$^6$Li | 24 | 1.18 |
| $^6$Li | $-0.016 \pm 0.006$ | $-0.018 \pm 0.002$ | $0.27 \pm 0.15$ | $^{40}$Ca/$^6$Li | 24 | 1.20 |
| $^9$Be | $-0.030 \pm 0.005$ | $-0.018 \pm 0.003$ | $0.40 \pm 0.11$ | $^9$Be/$^{12}$C | 15 | 0.22 |
| $^{12}$C | $-0.044 \pm 0.006$ | $-0.026 \pm 0.002$ | $0.33 \pm 0.04$ | $^{12}$C/$^2$D | 47 | 1.61 |
| $^{27}$Al | $-0.073 \pm 0.008$ | $-0.045 \pm 0.004$ | $0.81 \pm 0.32$ | $^{27}$Al/$^{12}$C | 15 | 0.48 |
| $^{40}$Ca | $-0.074 \pm 0.007$ | $-0.045 \pm 0.003$ | $0.68 \pm 0.10$ | $^{40}$Ca/$^2$D | 32 | 2.05 |
| $^{56}$Fe | $-0.089 \pm 0.011$ | $-0.057 \pm 0.006$ | $1.26 \pm 0.47$ | $^{56}$Fe/$^{12}$C | 15 | 0.72 |
| $^{64}$Cu | $-0.101 \pm 0.017$ | $-0.068 \pm 0.009$ | $0.91 \pm 0.35$ | $^{64}$Cu/$^2$D | 10 | 0.82 |
| $^{118}$Sn | $-0.100 \pm 0.004$ | $-0.060 \pm 0.002$ | $0.65 \pm 0.08$ | $^{118}$Sn/$^{12}$C | 161 | 0.74 |
| $^{208}$Pb | $-0.104 \pm 0.025$ | $-0.032 \pm 0.013$ | $0.99 \pm 0.32$ | $^{208}$Pb/$^2$D | 19 | 0.73 |
| $^{208}$Pb | $-0.124 \pm 0.012$ | $-0.074 \pm 0.006$ | $2.70 \pm 1.07$ | $^{208}$Pb/$^{12}$C | 13 | 0.22 |

unlike previous analyses. Third, we performed the fit over the entire $x$ range, while previous analyses [54, 56] were performed in restricted kinematical regions ($x < 0.1$ and $x < 0.7$, respectively). Moreover, both these earlier fits were performed with $\delta^A_{NS}$ corresponding to the study in [57, 58, 59]. In contrast, here, we extracted $\delta^A_{NS}$ values independently using an extremely extended data set. Nevertheless, the strong difference in determined $\delta^A_-$ and $\delta^A_{NS}$ leads to only modest differences in the nuclear modification factor $R^A$ (see below).

Now we turn to investigation of the nuclear dependence of the rescaling parameters $\delta^A_\pm$ and $\delta^A_{NS}$. Such dependence of nuclear scaling variables is often assumed to be proportional to $A^{1/3}$. However, there are approaches where much stronger, proportional to $A^{2/3}$, weaker, proportional to $A^n$ with $n \ll 1/3$, or even logarithmic $A$-dependencies[1)] are favored (see, for example, [37, 88–94], recent review [4] and references therein). We apply all $A$ dependences of nuclear modification considered earlier to the $A$ dependence of the rescaling parameters $\delta^A_\pm$ and $\delta^A_{NS}$. Therefore, we try to parametrize $A$ dependence of $\delta^A_\pm$ and $\delta^A_{NS}$ in several ways, namely,

$$\delta^A_i = a_i(A^{1/3} - 1), \tag{26}$$

$$\delta^A_i = a_i \ln A, \tag{27}$$

$$\delta^A_i = a_i(A^{1/3} - 1) + b_i(A^{-1/3} - 1), \tag{28}$$

where $i = \pm$ or $NS$, and we note that $\delta^A_\pm$ and $\delta^A_{NS}$ have to be zero at $A = 1$. Hereafter, the parameterizations in Eqs. (26), (27), and (28) are referred to as Fit A, Fit B, and Fit C, respectively. Based on the data from Table 1, we determine all parameters involved in the fits and list them in Table 2. The fitted nuclear dependence of $\delta^A_\pm$ and $\delta^A_{NS}$ is shown in Fig. 1. As can be seen from the Table 2 and Fig. 1, large uncertainties in the experimental data do not allow us to choose which of the parameterizations in Eqs. (26)–(28) is better. Thus, in accordance with the inaccuracies of the experimental data, each case from Eqs. (26)–(28) can be used for applications.

Having this dependence defined, the nuclear medium modification factor can be calculated for any nucleus $A$, even for unmeasured ones. This is demonstrated in Fig. 2, where the ratios $F_2^A(x,Q^2)/F_2^D(x,Q^2)$ for several nuclear targets are shown in comparison with available deep inelastic data. Note that some of these nuclei (for example, $^3$He, $^{14}$N, $^{108}$Ag, *etc.*) were not included into our fit due to insufficient statistics. For comparison, we present here the predictions obtained by the nIMP group [23], which are based on the dynamical parton model combined with some nuclear models. We find that predictions obtained with the parameterizations in Eqs. (26), (27), and (28) are close to each other and generally consistent with the experimental data. One can see that both nuclear dependence and $x$ dependence are more or less reproduced by our calculations. The strong rise of $F_2^A(x,Q^2)/F_2^D(x,Q^2)$ ratios at $x \geqslant 0.7$ is related to the consideration of Fermi motion in our analysis. A reasonably good description of the NMC data on the ratio of per-nucleon structure functions of one nucleus $A$ to another nucleus $A'$, $F_2^A(x,Q^2)/F_2^{A'}(x,Q^2)$, is achieved, as shown in Fig. 3. The

**Table 2.** Parameters $a_i$ and $b_i$ involved in the fits of the nuclear dependence of $\delta^A_\pm$ and $\delta^A_{NS}$ according to Eqs. (26), (27), and (28).

| | $a_+$ | $a_-$ | $a_{NS}$ | $b_+$ | $b_-$ | $b_{NS}$ |
|---|---|---|---|---|---|---|
| Fit A | $-0.027 \pm 0.001$ | $-0.015 \pm 0.002$ | $0.33 \pm 0.04$ | | | |
| Fit B | $-0.021 \pm 0.001$ | $-0.012 \pm 0.001$ | $0.25 \pm 0.04$ | | | |
| Fit C | $-0.020 \pm 0.004$ | $-0.012 \pm 0.002$ | $0.36 \pm 0.13$ | $0.029 \pm 0.015$ | $0.016 \pm 0.007$ | $0.12 \pm 0.54$ |

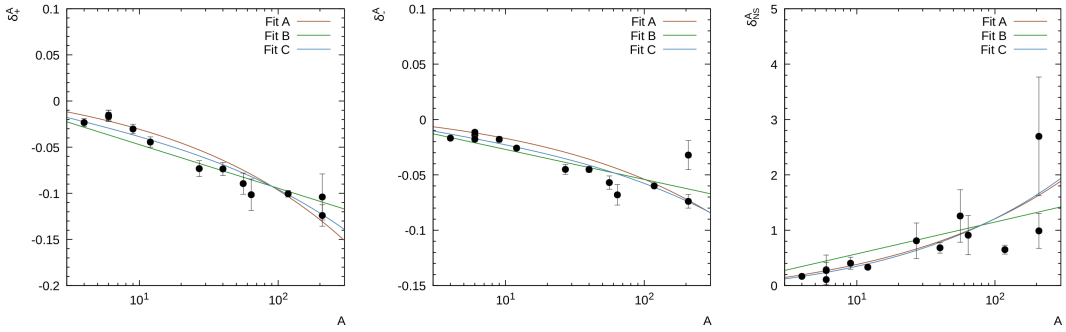


**Fig. 1.** (color online) Rescaling parameters $\delta^A_\pm$ and $\delta^A_{NS}$ listed in Table 1 and fitted accorgding to Eqs. (26), (27), and (28) as functions of mass number $A$.

1) The logarithmic $A$-dependence appeared, in particular, in the $x$-rescaling procedure [88].

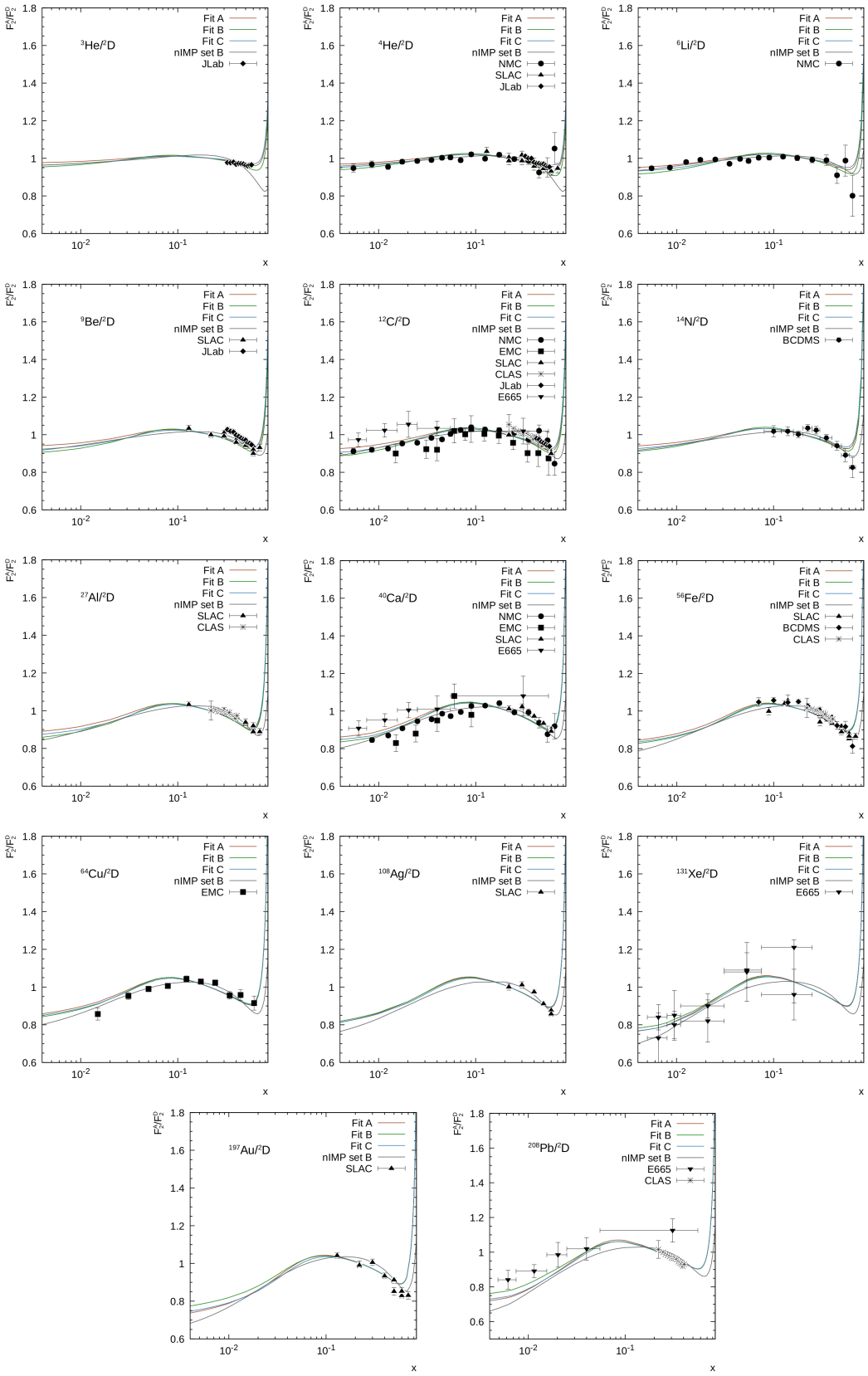


**Fig. 2.** (color online) Global fit results of structure function ratios $F_2^A(x,Q^2)/F_2^D(x,Q^2)$ between different nuclei targets $A$ and a deutron. Experimental data are from EMC [5−8], NMC [9−13], SLAC [14], BCDMS [15, 16], E665 [17, 18], JLab [19], and CLAS [20].

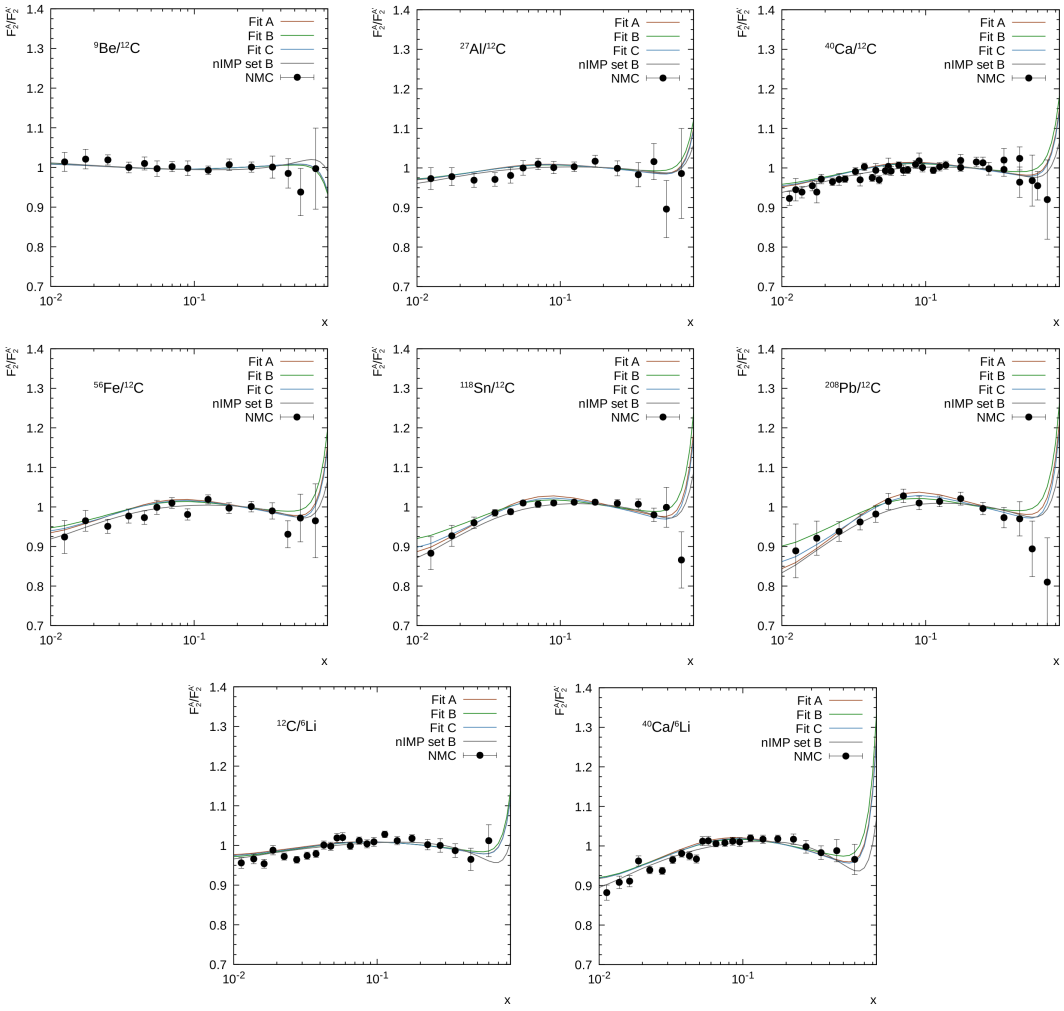


**Fig. 3.** (color online) Global fit results of structure function ratios $F_2^A(x,Q^2)/F_2^{A'}(x,Q^2)$ between different nuclei targets $A$ and $A'$. Experimental data are from NMC [9–13].

nuclear shadowing effect is described well by all the considered scenarios in Eqs. (26), (27), and (28). However, Fit A and Fit C as well as nIMP calculations [23] predict a slightly stronger shadowing for heavy nuclei compared to Fit B. Nevertheless, it is clear that more precise nuclear data, especially at low $x$, are necessary to distinguish between different approaches. Note that, for most of the data used, the points are taken for different $Q^2$; therefore, one should consider the lines depicted in Figs. 1 and 2 as interpolations in both $x$ and $Q^2$.

Next, using the analytical expressions in Eqs. (5)–(13) for the nucleon target, Eqs. (15)–(23) and (25) for nuclear targets, and fitted values of the rescaling parameters $\delta_{\pm}^A$ and $\delta_{NS}^A$ or rather their $A$-dependence, one can obtain predictions for the nuclear modification of parton distributions. Our results are shown in Fig. 4 for several light and heavy nuclei. As is well known, nuclear modification is weakly dependent on $Q^2$ at low and moderate $Q^2$; therefore, we show only the results for $Q^2 = 10$ GeV$^2$. For comparison, we also plot the results for gluon nuclear modification factors predicted by the nIMP group [23]. We find that the shadowing effect for gluons is, in general, weaker than for quarks, which is consistent with the results of other studies (see, for example, [23, 24, 37, 38]). Here, similar to structure function ratios, Fit A and Fit C predict slightly stronger (weaker) shadowing effects for heavy (light) nuclei compared to Fit B (see Fig. 1). Nevertheless, the difference between these results is rather small, and the predicted shadowing effects are close to the nIMP expectations. This is in contrast to the observations in the large-$x$ region, where we find a significant discrepancy with the nIMP calculations. In fact, the latter demonstrate a very weak antishadowing at $x \sim 0.1$, while our calculations indicate significant antishadowing effects for quarks. Note that a very large antishadowing of nuclear gluon densities is predicted by other groups [24, 38]. Thus, at present, it is difficult to draw any specific inference. We can conclude again that precision measurements at future colliders (EiC, EiCC) are needed to clarify this point. We hope that this analysis

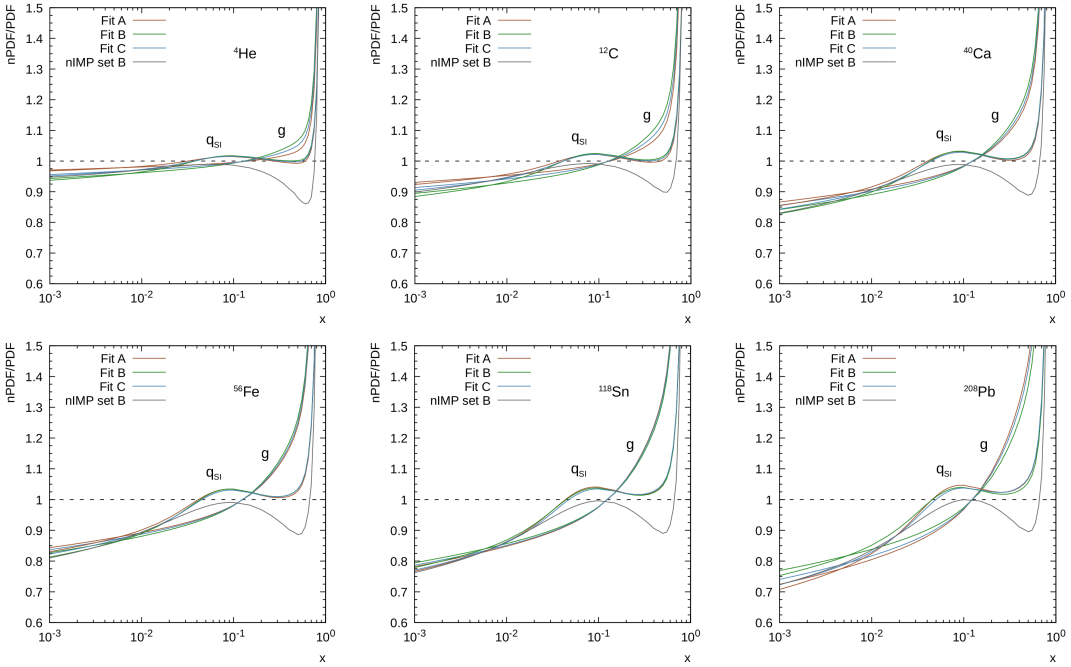


**Fig. 4.** (color online) The predicted nuclear modification factors for parton distributions in several nuclear targets. The results for gluon nuclear modification predicted by the nIMP group [23] are shown for comparison.

may simplify future comparisons between the experimental data and theory and could be helpful in distinguishing different approaches.

## V. CONCLUSION

In this work, we presented a brief overview of the nuclear medium modifications of parton densities based on the rescaling model. Moreover, we extended the rescaling model to include Fermi motion effects, providing a consistent description of nuclear modifications for DIS structure functions and parton distributions across the entire kinematic range. Using simple analytical formulas for proton PDFs derived at the LO of QCD coupling earlier, we performed a global analysis of available deep inelastic data for different nuclear targets and extracted the corresponding rescaling parameters $\delta^A_{\pm}$ and $\delta^A_{NS}$. Then, based on several assumptions about their nuclear dependence, we proposed a simple model to calculate the parton distributions for any nuclear target, even those not yet measured. Finally, the effects of nuclear modifications were investigated with respect to the mass number $A$. Our results highlight distinct shadowing and antishadowing behaviors for gluons and quarks, with implications for future studies of nPDFs with the NLO accuracy.

Note that, according to our current studies (see also [95]), in the rescaling model, the ratios of the valence and non-singlet parts of the parton densities in bound and free nucleons increase at small values of $x$. This contradicts the results of some other studies (see, for example, review [96]). Such a discrepancy can be eliminated by studying future experimental data for the DIS structure function $F_3(x,Q^2)$ in neutrino-nucleon and neutrino-nucleus scattering [84, 97, 98] (see also [4] and discussions therein). The structure function $F_3(x,Q^2)$ contains only the nonsinglet part, and thus, the corresponding ratio $R_3 = F_3^A(x,Q^2)/F_3(x,Q^2)$ should be greater than 1 at small $x$ in the rescaling model.

The developed approach can be easily used in different phenomenological applications. We hope that it will be also useful for future studies on lepton-nucleus, proton-nucleus, and nucleus-nucleus interactions at modern and future colliders, where nuclear parton dynamics could be examined directly.

## ACKNOWLEDGEMENTS

*We thank S. P. Baranov, H. Jung, and N. N. Nikolaev for their interest and important comments and remarks. In addition, we express our gratitude to M. A. Malyshev for reading our paper.*

## APPENDIX A: RESCALING MODEL

Here, we present the basic elements of the rescaling model [57−62]. We follow the recent preprint [99]. First, we consider the solution for the Mellin moments of the nonsinglet (NS) parton density at LO:

$$M_n^{\rm NS}(Q^2) = M_n^{\rm NS}(Q_0^2)\left[\frac{a_s(Q_0^2)}{a_s(Q^2)}\right]^{d_n^{\rm NS}} = M_n^{\rm NS}(Q_0^2)\left[\frac{\ln(Q^2/\Lambda^2_{\rm QCD})}{\ln(Q_0^2/\Lambda^2_{\rm QCD})}\right]^{d_n^{\rm NS}}, \quad d_n^{\rm NS} = \frac{\gamma_n^{\rm NS}}{2\beta_0}, \tag{A1}$$

where $\gamma_n^{\rm NS}$ is the LO NS anomalous dimension. The function $\ln M_n^{\rm NS}(Q^2)$ depends on $\ln[a_s(Q_0^2)/a_s(Q^2] \equiv s$ in the form of a straight line with the slope $d_n^{\rm NS}$. Experimental data confirm the behavior for each nucleus $A$; moreover, $M_n^{\rm A}(Q^2) < M_n^{\rm A'}(Q^2)$ for $A' > A$. Changing $Q^2 \to Q^2_{A'}(n) \equiv \xi_n^{AA'}(Q^2)\,Q^2$, we can obtain

$$M_n^{\rm A'}(Q^2) < M_n^{\rm A}\left(\xi_n^{AA'}(Q^2)Q^2\right) \tag{A2}$$

with $\xi_n^{AA'}(Q^2) > 1$ for $A' > A$ in the NS case. Then, using (A1), we have

$$M_n^{\rm A}\left(\xi_n^{AA'}(Q^2)Q^2\right) = M_n^{\rm A}\left(\xi_n^{AA'}(Q_0^2)Q_0^2\right)\left[\frac{a_s\left(\xi_n^{AA'}(Q_0^2)Q_0^2\right)}{a_s\left(\xi_n^{AA'}(Q^2)Q^2\right)}\right]^{d_n^{\rm NS}}, \tag{A3}$$

which is equal to

$$M_n^{\rm A'}(Q^2) = M_n^{\rm A'}(Q_0^2)\left[\frac{a_s(Q_0^2)}{a_s(Q^2)}\right]^{d_n^{\rm NS}}. \tag{A4}$$

Comparing the last two equations, we obtain

$$\frac{a_s\left(\xi_n^{AA'}(Q^2)Q^2\right)}{a_s\left(\xi_n^{AA'}(Q_0^2)Q_0^2\right)} = \frac{a_s(Q^2)}{a_s(Q_0^2)}. \tag{A5}$$

At LO, $a_s(\xi Q^2) = a_s(Q^2)/(1+\beta_0 a_s(Q^2)\ln\xi)$; therefore, we have

$$\frac{1+\beta_0 a_s(Q_0^2)\ln\xi_n^{AA'}(Q_0^2)}{1+\beta_0 a_s(Q^2)\ln\xi_n^{AA'}(Q^2)} = 1, \tag{A6}$$

or

$$\xi_n^{AA'}(Q^2) = \xi_n^{AA'}(Q_0^2)^{a_s(Q_0^2)/a_s(Q^2)}. \tag{A7}$$

A crucial observation was made in [61, 62] (see also [57, 58, 59]): $\xi_n^{AA'}(Q^2)$ is independent of $n$, *i.e.*, $\xi_n^{AA'}(Q^2) = \xi^{AA'}(Q^2)$. Thus, it is the same for all Mellin moments and even for the parton density itself. Thus, in the NS case, we have

$$f_{\rm A}^{\rm NS}(x,Q^2) = f^{\rm NS}\left(x,\xi_{\rm NS}^{AA'}(Q^2)Q^2\right), \tag{A8}$$

that is, the parton densities in the nucleus and the nucleon are related in a very simple manner within the framework of the rescaling model.

Note that the property in Eq. (A7) is not convenient for applications and can be simplified (see [54]). Consider $\ln\left[\xi^{AA'}\left(Q^2\right)Q^2\right)/\Lambda^2_{\rm QCD}] = \ln\left[\xi^{AA'}(Q^2)\right] + \ln\left[Q^2/\Lambda^2_{\rm QCD}\right]$, where

$$\ln\xi^{AA'}(Q^2) = \frac{a_s(Q_0^2)}{a_s(Q^2)}\ln\xi^{AA'}(Q_0^2) = \frac{\ln[Q^2/\Lambda^2_{\rm QCD}]}{\ln[Q_0^2/\Lambda^2_{\rm QCD}]}\ln\xi^{AA'}(Q_0^2). \tag{A9}$$

Thus, we have

$$\ln\left[\xi^{AA'}(Q^2)Q^2/\Lambda^2_{\rm QCD}\right] = \ln\left[Q^2/\Lambda^2_{\rm QCD}\right]\left(1+\frac{\ln\xi_n^{AA'}(Q_0^2)}{\ln\left[Q_0^2/\Lambda^2_{\rm QCD}\right]}\right) = \ln\left[Q^2/\Lambda^2_{\rm QCD}\right]\left(1+\delta^{AA'}\right), \tag{A10}$$

where

$$\delta^{AA'} = \frac{\ln\xi^{AA'}(Q_0^2)}{\ln\left[Q_0^2/\Lambda^2_{\rm QCD}\right]} = \beta_0 a_s(Q_0^2)\ln\xi^{AA'}(Q_0^2). \tag{A11}$$

The coefficient $\delta^{AA'}$ combines the normalization of the strong coupling $a_s(Q_0^2)$ and shift $\xi^{AA'}(Q_0^2)$ of the normalization argument when we move from $A$ kernels to $A'$ kernels. In a way, this is similar to introducing the $\Lambda_{\rm QCD}$ parameter:

$$a_s(Q^2) = \frac{a_s(Q_0^2)}{1+\beta_0 a_s(Q_0^2)\ln(Q^2/Q_0^2)} = \frac{1}{\beta_0 a_s(Q_0^2)\ln(Q^2/\Lambda^2_{\rm QCD})}, \tag{A12}$$

which accounts for both the normalization of the strong coupling $a_s(Q_0^2)$ and the normalization argument $Q_0^2$.

The variable $s^{A'} = \ln\left(\ln\left[\xi_n^{AA'}(Q^2)Q^2/\Lambda^2\right]/\ln\left[Q_0^2/\Lambda^2\right]\right) = s + \ln\left(1+\delta^{AA'}\right)$. When $A$ is a nucleon (and $A' \to A$), we have $s^A = s + \ln\left(1+\delta^{NA}\right)$; therefore, we reproduce Eq. (16) with $\delta^{NA} = \delta^A$.

In the NS case under consideration, we have $\xi^{NA}(Q_0^2) > 1$ and $\delta^{NA}_{NS} \equiv \delta^A_{NS} > 0$. Thus, $\delta^A_{NS}$ is a macroscopic characteristic of the evolution of the NS quark density in nuclei, which transforms it into nucleon parton density at higher values of $Q^2$.

Now, we consider the singlet quark and gluon densities, which obey the DGLAP equations. After diagonalization, the corresponding diagonal ± moments have the following form:

$$M_n^{\pm}(Q^2) = M_n^{\pm}(Q_0^2)\left[\frac{\ln(Q^2/\Lambda^2_{\rm QCD})}{\ln(Q_0^2/\Lambda^2_{\rm QCD})}\right]^{d_n^{\pm}}, \quad d_n^{\pm} = \frac{\gamma_n^{\pm}}{2\beta_0}, \tag{A13}$$

where diagonal anomalous dimensions $\gamma_n^{\pm}$ are

$$\gamma_n^{\pm} = \gamma_n^{gg} - \gamma_n^{qq} \pm \sqrt{(\gamma_n^{gg} - \gamma_n^{qq})^2 + 4\gamma_n^{gq}\gamma_n^{qg}} \tag{A14}$$

and $\gamma_n^{ab}$ are the LO parton anomalous dimensions. Therefore, the result in Eq. (A14) is similar to that in Eq. (A1).

The "+" component contains singular terms at $n \to 1$ , and thus, it provides dominant contributions in the low $x$ range. Therefore, the shadowing effect can be interpreted within the framework of the rescaling model as a change in scale with $\xi_+^{AA'}(Q^2) < 1$, and thus, $\delta_+^A < 0$. The "−" component, along with the "+" and NS components, is important at $x \sim 0.1 \ldots 0.2$, and thus, all these components are responsible for the possible antishadowing effect. In the pure rescaling model, antishadowing should occur due to momentum conservation, because $R^A < 1$ at $x \geqslant 0.3$ and $x \leqslant 0.1$. In the case under consideration, where we also took Fermi motion into account, $R^A > 1$ for $x \geqslant 0.7$. Thus, the antishadowing effect may or may not manifest itself. Thus, there are no strict restrictions for the value of $\delta_-^A$, and its value should be obtained from the data.

## References


[1] M. Arneodo, Phys. Rep. **240**, 301 (1994)
[2] P. R. Norton, Rep. Prog. Phys. **66**, 1253 (2003)
[3] S. Malace, D. Gaskell, D. W. Higinbotham *et al.*, Int. J. Mod. Phys. E **23**, 1430013 (2014)
[4] M. Klasen and H. Paukkunen, Ann. Rev. Nucl. Part. Sci. **74**, 49 (2024)
[5] EMC Collaboration, Phys. Lett. B **202**, 603 (1988)
[6] EMC Collaboration, Phys. Lett. B **211**, 493 (1988)
[7] EMC Collaboration, Nucl. Phys. B **333**, 1 (1990)
[8] EMC Collaboration, Z. Phys. C **57**, 211 (1993)
[9] NMC Collaboration, Z. Phys. C **53**, 73 (1992)
[10] NMC Collaboration, Nucl. Phys. B **441**, 3 (1995)
[11] NMC Collaboration, Nucl. Phys. B **441**, 12 (1995)
[12] NMC Collaboration, Nucl. Phys. B **481**, 3 (1996)
[13] NMC Collaboration, Nucl. Phys. B **481**, 23 (1996)
[14] J. Gomes *et al.*, Phys. Rev. D **49**, 4348 (1994)
[15] BCDMS Collaboration, Phys. Lett. B **163**, 282 (1985)
[16] BCDMS Collaboration, Phys. Lett. B **189**, 483 (1987)
[17] E665 Collaboration, Z. Phys. C **67**, 403 (1995)
[18] E665 Collaboration, Phys. Rev. Lett. **68**, 3266 (1992)
[19] J. Seely *et al.*, Phys. Rev. Lett. **103**, 202301 (2009)
[20] CLAS Collaboration, Nature **566**, 354 (2019)
[21] S. I. Alekhin, S. A. Kulagin, and R. Petti, Phys. Rev. D **105**, 114037 (2022)
[22] S. I. Alekhin, S. A. Kulagin, and R. Petti, Phys. Rev. D **96**, 054005 (2017)
[23] R. Wang, X. Chen, and Q. Fu, Nucl. Phys. B **920**, 1 (2017)
[24] R. A. Khalek, R. Gauld, T. Giani *et al.*, Eur. Phys. J. C **82**, 507 (2022)
[25] S. A. Kulagin, EPJ Web Conf. **138**, 01006 (2017)
[26] EMC Collaboration, Phys. Lett. B **123**, 275 (1983)
[27] L. Stodolsky, Phys. Rev. Lett. **18**, 135 (1967)
[28] V. N. Gribov, Zh. Eksp. Teor. Fiz. **57**, 1306 (1969)
[29] N. N. Nikolaev and V. I. Zakharov, Phys. Lett. B **55**, 397 (1975)
[30] V. I. Zakharov and N. N. Nikolaev, Sov. J. Nucl. Phys. **21**, 227 (1975)
[31] N. N. Nikolaev and B.G. Zakharov, Z. Phys. C **49**, 607 (1991)
[32] N. N. Nikolaev, Sov. Phys. Usp. **24**, 531 (1981)
[33] V. N. Gribov and L. N. Lipatov, Sov. J. Nucl. Phys. **15**, 438 (1972)
[34] L. N. Lipatov, Sov. J. Nucl. Phys. **20**, 94 (1975)
[35] G. Altarelli and G. Parisi, Nucl. Phys. B **126**, 298 (1977)
[36] Yu. L. Dokshitzer, Sov. Phys. JETP **46**, 641 (1977)
[37] A. W. Denniston, T. Jezo, A. Kusina *et al.*, Phys. Rev. Lett. **133**, 152502 (2024)
[38] K. J. Eskola, P. Paakkinen, H. Paukkunen *et al.*, Eur. Phys. J. C **82**, 413 (2022)
[39] P. Duwentäster, T. Ježo, M. Klasen *et al.*, Phys. Rev. D **105**, 114043 (2022)
[40] H. Khanpour, M. Soleymaninia, S. A. Tehrani *et al.*, Phys. Rev. D **104**, 034010 (2021)
[41] I. Helenius, M. Walt, and W. Vogelsang, Phys. Rev. D **105**, 094031 (2022)
[42] R. Wang, R. Dupre, Y. Huang *et al.*, Phys. Rev. C **99**, 035205 (2018)
[43] C. A. Garcia Canal *et al.*, Phys. Rev. Lett. **53**, 1430 (1984)
[44] M. Staszel, J. Rozynek, and G. Wilk, Phys. Rev. D **29**, 2638 (1984)
[45] S. V. Akulinichev, S. Shlomo, S. A. Kulagin *et al.*, Phys. Rev. Lett. **55**, 2239 (1985)
[46] L. L. Frankfurt and M. I. Strikman, Phys. Lett. B **183**, 254 (1987)
[47] H. Jung and G. A. Miller, Phys. Lett. B **200**, 351 (1988)
[48] C. Ciofi degli Atti, L. P. Kaptari, and S. Scopetta, Eur. Phys. J. A **5**, 191 (1999)
[49] G. V. Dunne and A. W. Thomas, Phys. Rev. D **33**, 2061 (1986)
[50] F. Gross and S. Liuti, Phys. Rev. C **45**, 1374 (1992)
[51] S. A. Kulagin, G. Piller, and W. Weise, Phys. Rev. C **50**, 1154 (1994)
[52] S. A. Kulagin and R. Petti, Nucl. Phys. A **765**, 126 (2006)
[53] S. A. Kulagin and R. Petti, Phys. Rev. C **90**, 045204 (2014)
[54] A.V. Kotikov, B. G. Shaikhatdenov, and P. M. Zhang, Phys. Rev. D **96**, 114002 (2017)
[55] A. V. Kotikov, B. G. Shaikhatdenov, and P. M. Zhang, Phys. Part. Nucl. Lett. **16**, 311 (2019)
[56] A.V. Kotikov, A.V. Lipatov, and P. M. Zhang, JETP. Lett. **119**, 745 (2024)
[57] R. L. Jaffe, F. E. Close, R. G. Roberts *et al.*, Phys. Lett. B **134**, 449 (1984)
[58] O. Nachtmann and H. J. Pirner, Z. Phys. C **21**, 277 (1984)
[59] F. E. Close, R. L. Jaffe, R. G. Roberts *et al.*, Phys. Rev. D **31**, 1004 (1985)
[60] F. E. Close, R. G. Roberts, and G. G. Ross, Nucl. Phys. D **296**, 582 (1988)
[61] F. E. Close, R. G. Roberts, and G. G. Ross, Phys. Lett. B **129**, 346 (1983)
[62] R. L. Jaffe, Phys. Rev. Lett. **50**, 228 (1983)
[63] M. Hirai, S. Kumano, and T.-H. Nagai, Phys. Rev. C **70**, 04495 (2004)
[64] M. Hirai, S. Kumano, and T.-H. Nagai, Phys. Rev. C **76**, 065207 (2007)
[65] K. J. Eskola, Nucl. Phys. A **910**, 163 (2013)

[66] V. Barone, Z. Phys. C **58**, 541 (1993)
[67] N. A. Abdulov, A.V. Kotikov, and A.V. Lipatov, Phys. Part. Nucl. Lett. **20**, 557 (2023)
[68] A.V. Kotikov and A.V. Lipatov, Phys. Rev. D **111**, 094009 (2025)
[69] N. A. Abdulov, A.V. Kotikov, and A.V. Lipatov, Particles **5**, 535 (2022)
[70] A.Yu. Illarionov, A.V. Kotikov, S. S. Parzycki *et al*., Phys. Rev. D **83**, 034014 (2011)
[71] C. Lopez and F. J. Yndurain, Nucl. Phys. B **171**, 231 (1980)
[72] NMC Collaboration, Phys. Rev. D **50**, R1 (1994)
[73] A. V. Kotikov, V. G. Krivokhizhin, and B. G. Shaikhatdenov, Phys. Atom. Nucl. **81**, 244 (2018)
[74] A.V. Kotikov and G. Parente, Nucl. Phys. B **549**, 242 (1999)
[75] A.Yu. Illarionov, A.V. Kotikov, and G. Parente, Phys. Part. Nucl. **39**, 307 (2008)
[76] L. Mankiewicz, A. Saalfeld, and T. Weigl, Phys. Lett. B **393**, 175 (1997)
[77] A. De Rujula, S. L. Glashow, H. D. Politzer *et al*., Phys. Rev. D **10**, 1649 (1974)
[78] C. Lopez and F. J. Yndurain, Nucl. Phys. B **183**, 157 (1981)
[79] N. N. Nikolaev and B. G. Zakharov, Phys. Lett. B **327**, 157 (1994)
[80] B. Escoubes, M. J. Herrero, C. Lopez *et al*., Nucl. Phys. B **242**, 329 (1984)
[81] A. Bodek and J. L. Ritchie, Phys. Rev. D **23**, 1070 (1981)
[82] L. L. Frankfurt and M. I. Strikman, Nucl. Phys. B **181**, 22 (1981)
[83] M. Wang, G. Audi, A. H. Wapstra *et al*., Chin. Phys. C **36**, 1603 (2012)
[84] Particle Data Group Collaboration, Phys. Rev. D **110**, 030001 (2024)
[85] A.V. Kotikov, A.V. Lipatov, and N. P. Zotov, JETP **101**, 811 (2005)
[86] G. Cvetic, A. Yu. Illarionov, B. A. Kniehl *et al*., Phys. Lett. B **679**, 350 (2009)
[87] www.gnuplot.info.
[88] E. P. Segarra, T. Ježo, A. Accardi *et al*., Phys. Rev. D **103**, 114015 (2021)
[89] L. D. McLerran and R. Venugopalan, Phys. Rev. D **49**, 2233 (1994)
[90] L. D. McLerran and R. Venugopalan, Phys. Rev. D **49**, 3352 (1994)
[91] A. H. Mueller, Nucl. Phys. A **724**, 223 (2003)
[92] K. Rummukainen and H. Weigert, Nucl. Phys. A **739**, 183 (2004)
[93] Y. V. Kovchegov, Phys. Rev. D **61**, 074018 (2000)
[94] E. Levin and K. Tuchin, Nucl. Phys. B **573**, 833 (2000)
[95] A.V. Kotikov, Sov. J. Nucl. Phys. **50**, 127 (1989)
[96] S. A. Kulagin, J. Phys. Conf. Ser. **762**, 012072 (2016)
[97] M. Hirai, S. Kumano, and T. H. Nagai, Phys. Rev. D **71**, 113007 (2005)
[98] K. J. Escola and H. Paukkunen, JHEP **2006**, 008 (2006)
[99] R. L. Jaffe, arXiv: 1811.05615 [hep-ph]